20

Commercial magnetometers and their application

D. C. Hovde, M. D. Prouty, I. Hrvoic, and R. E. Slocum

20.1 Introduction

Applications such as geophysical exploration for minerals and oil, anti-submarine warfare, volcanology, earthquake studies, magnetic observatories, and the detection of buried objects at sites of archaeological significance require instruments that can measure small variations of the Earth's magnetic field in time and space. Other applications such as laboratory metrology, space exploration, and biomedicine may require measurements at lower or higher fields. The demand for precise measurements of magnetic fields is met in part by commercial atomic magnetometers supplied by a number of manufacturers over the last fifty years. Commercial optical magnetometers based on cesium, potassium, and helium are now firmly established. Commercial magnetometers designed for measuring anomalies in the Earth's field are typically operated as self-oscillating devices or VCO (voltage-controlled oscillator) lock-in devices with the oscillation or lock-in frequency proportional to the magnetic field. This chapter examines the specifications for atomic magnetometers, compares the most widely used approaches, describes some of the features demanded by different applications, and surveys the history of atomic magnetometers. (The online supplemental material contains a table listing many of the United States patents related to the field of atomic magnetometry.)

Earth's field at the surface ranges from 20 to 80 μT. Typically the user is seeking to generate a map of the local magnetic field upon which magnetic anomalies can be discerned. The map may be made by means of a walking survey, for instance in the case of archaeological sites. For mineral exploration much wider areas must be surveyed, so that typically airborne and ground surveys are required. The magnetic anomalies can be in the pT range or even smaller. For such applications, the most significant requirement for the magnetometer is its sensitivity. Because the fluctuations of Earth's field are in the range of 100 nT or even greater, applications may require differential methods such as gradiometers

Optical Magnetometry, ed. Budker, D. and Jackson Kimball, D. F. Published by Cambridge University Press.

(two or more magnetometers whose difference is measured during the survey) or a single moving magnetometer in tandem with a fixed "base station" that is used to correct the long-scale fluctuations seen by the mapping magnetometer. In either case, because the magnetometer moves as the map is generated, heading-error effects are also important. Other applications, such as magnetic observatories or long-term studies, require absolute accuracy and freedom from slow drifts. Often the orientation of the magnetometer is fixed for these applications. Reliability, cost, size, power, weight, and other features such as the ability to export data to standard mapping programs also impact the commercial success of atomic magnetometers.

20.2 Specifications

20.2.1 Noise

Noise, by definition, is any variation in the measurement not caused by actual variations in the external magnetic field. Sources of noise in the magnetometer include quantum shot noise, excess noise from the electronics, and eddy currents and other technical noise sources from the sensor. Noise is specified for a fixed sensor, so that the heading or motion errors are not included in the background system-noise specification.

Noise is normally specified in nanoteslas (10^{-9} T) per square root hertz (nT/$\sqrt{\text{Hz}}$) or in some cases picoteslas (10^{-12} T) per square root hertz (pT/$\sqrt{\text{Hz}}$). The frequency in hertz (Hz) refers to the measurement bandwidth rather than to the Larmor frequency. The bandwidth is not simply the inverse of the sampling rate or measurement cycle time, but includes electronic bandwidth, oversampling, and Nyquist effects. Although peak-to-peak noise measurements have been used, more typically the measurements are reported as root mean squared (RMS), as the RMS has a more rigorous statistical definition than peak-to-peak.

Magnetometer noise does not always scale as the square root of the sample rate or bandwidth. The actual scaling depends on the time scale of the measurement (compared to the time scale of the underlying atomic polarization being measured) and on the electronics used to measure the Larmor frequency. Magnetic field amplitude is measured by counting precession frequency cycles during the measurement time. Simultaneously, time is measured by counting a much higher frequency internal clock. The precession frequency can be inferred from the change in the phase $\Delta\phi$ over the counting interval Δt:

$$\Omega = \frac{\Delta\phi}{\Delta t} . \tag{20.1}$$

With the simplest counter circuitry, the start time is determined from a single zero crossing, and likewise for the stop time. The counter counts cycles that differ in phase by 2π. The precession frequency is given by

$$\Omega = \frac{2\pi n_{\text{cycles}}}{\Delta t} . \tag{20.2}$$

The numerator is 2π times an integer with no uncertainty in normal operation (although missing counts may occur and can be corrected for). Over short time scales, uncertainty in the frequency therefore arises from estimating the start and stop times for the interval:

$$\left(\frac{\sigma_\Omega}{\Omega}\right)^2 = \left(\frac{\sigma_{\Delta t}}{\Delta t}\right)^2. \tag{20.3}$$

The uncertainty in time depends on the slope and noise of the Larmor waveform at the two crossings. These are independent of the measurement interval Δt; so the uncertainty in Ω, and hence magnetic field noise reported by the sensor, scales as $1/\Delta t$. Graphically, this is equivalent to determining the slope of the line $\phi(t)$ from the phase measurements at the beginning and end of the measurement time, without using any of the data in between.

However, it is possible to measure the frequency from all n zero crossings within the measurement time by finding the best-fit line to each of the n zero crossings within the measurement time. This could be implemented in hardware with a phase-locked loop limited in bandwidth. As a result of the additional phase data, the uncertainty in the magnetic field decreases by an extra factor of $1/\sqrt{\Delta t}$, for an overall factor of $1/\Delta t^{3/2}$. The overall result is that the noise of a commercial magnetometer at short measurement times scales as the measurement bandwidth to the 3/2 power. In this discussion the magnetic field is assumed to be constant over the course of the measurement, so that the fluctuations are due to noise alone. The effects of narrow-band filters such as phase-locked loops are discussed below in the section on bandwidth (Section 20.2.5).

While noise affects the counter directly, over longer time scales it also affects the operation of the self-oscillating or VCO lock-in loop. Noise near the precession frequency adds to the measured phase, and the feedback loop adjusts the frequency slightly to cancel the phase noise. The result is Brownian diffusion of the phase of the oscillator, which gives rise to noise proportional to $1/\sqrt{t}$ when the system is observed for times long compared to the atomic-coherence time [1].

When a manufacturer does not specify a measurement bandwidth for the noise, but instead provides an absolute noise in nT, the reader should assume the specification is valid only at the slowest cycle rate of the system, i.e., several seconds or more.

The noise of a magnetometer is typically determined from measurements taken over time scales appropriate for the frequency range of interest – usually on the order of a few minutes. In practice there are three methods used to measure the sensitivity of commercial magnetometers:

1. Comparison of readings of two co-located magnetometers in a magnetic field that is sufficiently quiet that the gradients are constant. Most manufacturers maintain a magnetically quiet test site in a rural area for purposes of testing magnetometers at the $\mathrm{pT}/\sqrt{\mathrm{Hz}}$ sensitivity and better. The time intervals of the readings of the two magnetometers are strictly synchronized. Typically a few hundred readings (when determining the short-term sensitivity) are recorded. The difference of readings is taken and the RMS

value of its scatter is calculated. Since this represents noise of two equal, independent, and uncorrelated magnetometers, the noise has to be divided by the square root of 2. This method assumes a stable gradient between the two sensor positions.

2. Measurement in a quiet magnetic field. If the magnetic field can be stabilized more accurately than the expected noise of the magnetometer under test, one can take a sufficient number of readings in this stable field and compute the RMS value of the scatter. Magnetic shields (Chapter 12) can be used to produce a magnetically quiet region, inside which a DC field can be generated by means of suitable coils. However, the noise of typical current sources makes this method difficult to apply to the best commercial magnetometers. A current source used to produce a field of 50 μT, typical of Earth's surface, must be stable to 1 part in 10^8 in order to keep current noise from dominating the measurement. Gradient measurements with two magnetometers inside the shields can ease the requirements on the current source.
3. Recording a time series and processing it to determine the power spectral distribution of the field can refine the measurements in a quiet field. Such a time series and related power spectral distribution are shown in Figs. 20.1 and 20.2, for signals from a single magnetometer recorded in a magnetic shield. Strong structure from power lines (at 60 Hz) is present, even in a well-shielded location. At the low-frequency end, below 1 Hz and lower frequencies, fluctuations in the applied field dominate the spectrum. White noise from the instrument is probably the limiting factor near 5 Hz.

For measurements of magnetic anomalies, long-term sensitivity or long-term stability of magnetometers is not important. For magnetic observatories, volcanology, earthquake

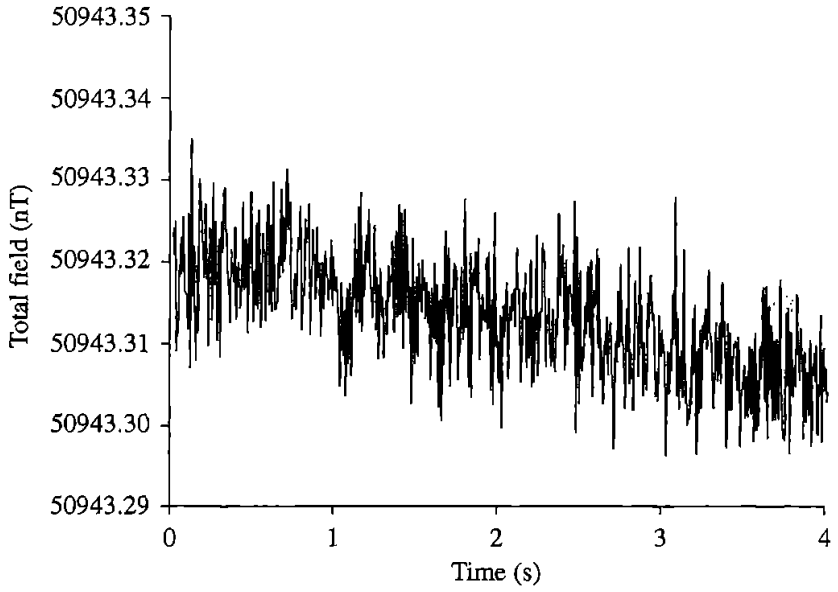

Figure 20.1 Four seconds of magnetic field as a function of time, measured inside high-quality shields. The magnetic field was updated every 4 ms, resulting in a Nyquist limit of 125 Hz.

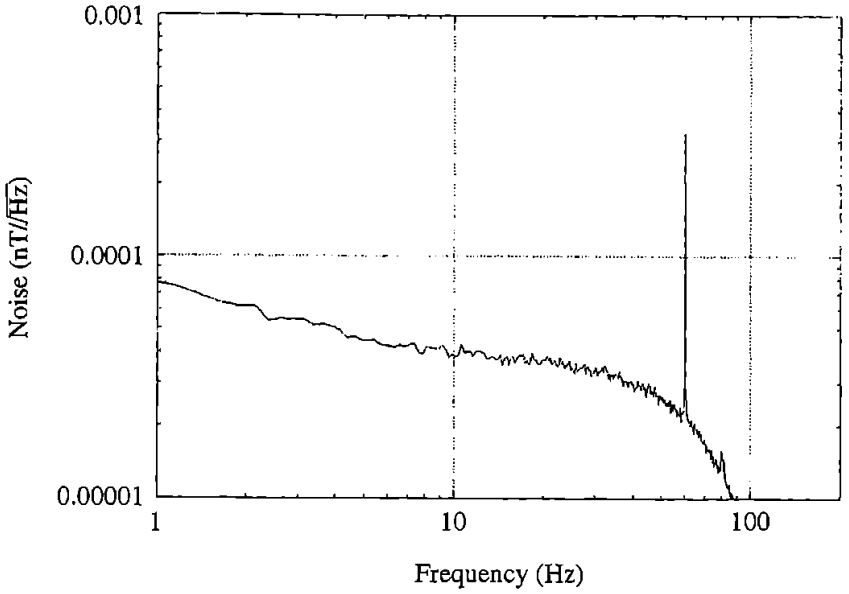

Figure 20.2 The power spectral distribution determined from 450 seconds of field data including the portion shown in Fig. 20.1. Note the 60 Hz noise spike. An additional spike at 90 Hz arises from the presence within the shields of a second magnetometer. Gradients within the shields result in a difference in Larmor frequencies of 90 Hz. (Data provided courtesy of Geometrics.)

studies, and space measurements, on the other hand, long-term stability can be very important. Long-term stability may differ substantially from the short-term sensitivity discussed above.

20.2.2 Resolution

The resolution of a magnetometer is the smallest change in magnetic field the magnetometer can resolve or report. The resolution may not be equal to the least-significant digit of the instrument's readout at all settings. The user should choose a magnetometer which has a counter resolution smaller than the smallest change in magnetic field being detected, or "quantization errors" will result, improperly defining the shape and character of the anomaly. Because the resolution of a magnetometer usually varies with sample rate, it is important to make sure that the resolution specification applies to the intended sample rate.

20.2.3 Sensitivity

The term "sensitivity" is a common specification offered for commercial magnetometers but because manufacturers define the term differently it makes for a difficult comparison. Sensitivity can be defined as the larger of either the resolution or the noise. With this definition, the sensitivity specification provides a single number that can be used for performance comparison between magnetometers that are limited by their resolution and those that are limited by their noise. The manufacturer should specify sensitivity for all expected speeds

Table 20.1. *Typical sensitivity at 1 Hz bandwidth for various commercial magnetometers.*

Atom	Sample size (mm)	Sensitivity (pT)
K	35	0.5
K	70	0.1
K	150	0.03
Cs	25	0.5
He-4	20	0.3
He-4	75	0.04
He-3	20	1.0

of reading and associated bandwidths over a range of magnetic fields characteristic of the Earth and perhaps a range of temperatures.

Instrumental factors that affect the sensitivity include the size of the atomic vapor sample and the atomic medium. Larger samples result in a measurement that makes use of a greater number of spins. Optical depth can approach unity without introducing spin-relaxing collisions. Together these two factors reduce shot noise and improve sensitivity. Large sample volumes also reduce wall relaxation processes, which can result in narrower resonances and thus improved sensitivity. Table 20.1 shows representative sensitivity in a 1 Hz bandwidth and the sensor size for a number of vendors.

20.2.4 Sample rate and cycle time

Sample rate is defined as the number of readings per second generated by the magnetometer. It is often specified as a frequency of reading in Hz. Cycle time, the number of seconds per reading, is the inverse of the sample rate. When constructing a magnetic-anomaly map, the field has to be sampled at a suitable spatial scale. This spatial scale should be small compared to the depth of the targets in order for the survey to locate the target accurately. The cycle time of the magnetometer and the speed with which it is moved over the ground determine the distance between measurements. In hand-carried devices, the user can walk slowly to increase the data density, at the expense of reduced production. In airborne and marine applications, this option is often impractical, as the vehicle may have some minimum operating speed. In any case, the desired sample rate will affect the choice of bandwidth.

20.2.5 Bandwidth

The bandwidth of a magnetometer is a measure of how well it can respond to rapid changes in the measured field. Higher bandwidth allows a magnetometer to faithfully reproduce a rapidly fluctuating actual field. All digital magnetometers report a value based on an average

of the observed precession frequency during a "read" period. This value is normally the average value over a period less than or equal to the sample update time. In such cases, it is the sample rate and not any internal averaging that limits the frequency content of the data. In other cases where there are filters that average the frequency over longer times, these filters can become the limiting factor of frequency content.

The bandwidth of the magnetometer should be matched to the bandwidth of the magnetic field fluctuations of interest. When mapping out magnetic anomalies, the measurement bandwidth must be large enough to not distort the anomalies. If any significant processing of the data has been done inside the magnetometer, it is important to know the resulting bandwidth of the system because this determines the basic utility of the system. It is possible for example, to make smooth, low-variability magnetic data by applying a digital filter that removes all high frequencies from the output. Although the system appears to offer both low noise and rapid updates of the magnetic field, in fact such a filter removes both noise and any high-frequency content of the magnetic signal. In such cases it is the filter and not sample rate that determines the fastest speed at which a survey should be done. Over-filtering limits the performance of software that calculates the depth of targets and can mask the anomalies caused by small objects.

Commercial magnetometers are mixed analog-digital devices. The analog end can also include filtering. Narrow-band notch filters are not typically used, due to the wide range of frequencies over which the magnetometer must operate. A phase-locked loop can be used to reduce the noise bandwidth while preserving frequency agility. The time constant of the loop determines the noise bandwidth. The output can be digitized. Typically, the output is over-sampled to reduce aliasing. If the magnetic field has strong components near the Nyquist limit, then these may still be aliased down to the detection band. This problem can be detected as an anomalous increase of noise with the increase of the rate of readings.

20.2.6 Absolute error and drift

The absolute error is defined as the difference between the average of the readings of the magnetometer and the average of the field it measures. Drift is defined as the change in the absolute error with time. All magnetometers will have some absolute error and drift in their measurements. In most cases the drift will be much less than the absolute error.

For producing maps of magnetic anomalies, the drift specification is more important than the absolute error. For most surveys, a drift of less than 0.1 nT per day is acceptable. Greater drift than this causes noticeable artifacts such as survey block edge effects (i.e, discontinuities in the magnetic field map arising when adjacent regions are sampled at significantly different times). Because other survey errors (positional inaccuracies, heading errors due to internal instrument and mobile platform effects, diurnal Earth's field variations) usually dominate and are cumulative, absolute accuracies in the range of 2 to 4 nT are widely deemed acceptable. When a magnetometer is being used as a primary standard or in an observatory, then absolute accuracy and drift specifications are primary factors and sub-nT

absolute errors are required. Criteria for achieving good absolute accuracy are numerous [2]. The gyromagnetic ratio is known precisely for protons in water at 25°C. The International Association of Geomagnetism and Aeronomy recommends using the latest CODATA values for all measurements after 1992. The 2010 CODATA value for the proton gyromagnetic ratio [3] is $\gamma_p = 2.675\,222\,005(63) \times 10^8\ \mathrm{s^{-1}\,T^{-1}}$ (or $0.267\,522\,2005\ \mathrm{rad\,s^{-1}\,nT}$). The gyromagnetic ratio of the proton in water is slightly different due to the shielding effects of the induced magnetic fields. At 25°C in a spherical sample surrounded by vacuum, the accepted value for water [3] is $2.675\,153\,268(66) \times 10^8\ \mathrm{s^{-1}\,T^{-1}}$. An accurate determination of the magnetic field from the precession of Cs depends on the hyperfine level and the nonlinear Zeeman effect [4]. Although the underlying spectroscopy is almost as well known (the fine-structure g-factor is known to about 1 part in 10^7), atomic magnetometers that measure a poorly defined blend of hyperfine lines will not achieve the highest absolute accuracy.

20.2.7 Gradient tolerance

Gradient tolerance is defined as the ability of the magnetometer to obtain a meaningful reading in a given gradient, not necessarily with the highest sensitivity. When the field has large gradients, errors in assessing the position of the sensor may dominate the error budget, so an increase in noise may be tolerable. Gradient tolerance depends on both the spectral line width and the size of sensor – smaller sensors tend to have high gradient tolerance. Wider spectral lines (Cs, Rb, ^{4}He) tend to show better gradient tolerance, although if a buffer gas is used then collisions with the buffer gas slow the movement of the atoms and limit the magnetometer's tolerance for gradients. The effect of gradients has been studied in the laboratory on paraffin-coated cells [5]. For a potassium-based sensor without buffer gas, a cell with a diameter of 35 mm has been shown to operate at gradients of over 50 000 nT/m. Gradient tolerance falls off sharply with increased sensor size. A similar potassium cell with a diameter of 70 mm can operate only in gradients of up to 1 000 nT/m, while 150 mm cells cannot withstand any movement of the cell and tolerate perhaps a 100 nT/m gradient at maximum.

Gradient tolerance also depends on the distance the atoms can diffuse over the time scale of the coherence. Proton-precession and Overhauser-type magnetometers generate the Larmor signal from a liquid sample such as water or hydrocarbons. Typical gradient tolerance for proton magnetometers is in the range of 1 000 nT/m but may be less depending on the absolute field strength (lower fields produce lower signals in proton and Overhauser magnetometers, lowering their gradient tolerance in low-field areas such as Brazil).

Magnetic gradients reduce the amplitude of the magnetometer signal. This can result in increased noise, lower sensitivity, and increased dead zone. In applications such as airborne surveys, the sensor is far from field sources, so gradient tolerance is not an important specification. In surveys of unexploded ordnance or landfills, gradients can be very large, requiring a magnetometer that tolerates large gradients.

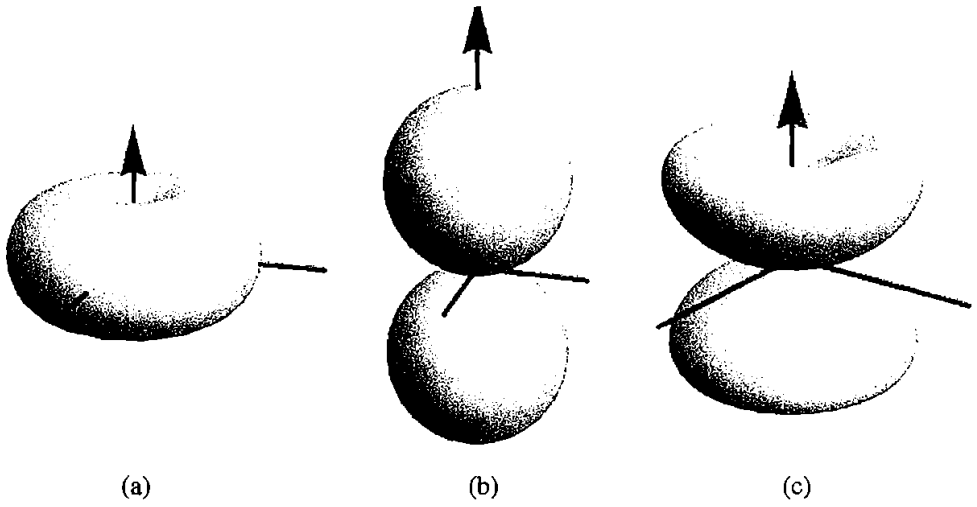

Figure 20.3 Polar plots showing signal strength for various sensor orientations with different types of dead zones: (a) a polar dead zone, (b) an equatorial dead zone, and (c) both (courtesy of Geometrics).

20.2.8 Dead zones

Atomic magnetometers have dead zones which occur when the orientation of the magnetometer is such that the signal is so weak that the magnetometer ceases to operate. The range of solid angles of the dead zone depends on the details of construction of the magnetometer, but the basic topology is a function of the underlying symmetry of the electromagnetic-field/atom system. Figure 20.3 shows dead zones associated with some commercial cesium magnetometer designs.

A number of ways exist to mitigate the problems with dead zones. In optically pumped systems an adjustable-orientation fixture can hold the sensor so that the sensor can be positioned such that it will not enter a dead zone during survey maneuvers. In proton-precession and Overhauser systems, dead zones can be eliminated with appropriate design. In some applications, the orientation of the optical sensor cannot be controlled. In such cases, it is necessary to have duplicate sensors oriented so that their dead zones do not overlap, or to choose a different measurement technology. ^{4}He magnetometers normally employ a design consisting of three integrated orthogonal sensor axes to achieve maximum sensitivity on all headings.

20.2.9 Heading error

Although scalar atomic magnetometers are designed to measure the total magnetic field, the field reported by a sensor depends slightly on its orientation in the field. This (unwanted) dependence of the measurement on orientation is termed heading error. Heading error is most important in airborne and marine systems and less so in hand-carried systems. This is because in airborne systems the aircraft must constantly change its orientation angle to maintain the correct path over the ground. In marine systems, the sensor undergoes some

change in orientation as it is towed. In land systems, heading error is less apparent as a person tends to hold a sensor at a more or less constant angle. When generating magnetic contour maps, the magnetometer typically reverses direction on each pass across the measurement zone; heading error will produce "striping" in the final result. There are methods for post-acquisition removal of this artifact, but a better course is to minimize the error by careful design of the instrument.

Manufacturers commonly specify the heading error for a sensor as a peak-to-peak value. Heading errors are measured by placing the test sensor on a rotation stage surrounded by one or two fixed witness sensors. The test sensor is rotated through its operating range while monitoring the signals of the rotating and fixed sensors. Then the deviation of the test sensor from the witness sensors is plotted as a function of angle. Ideally, the witness sensors should be close enough to one another and the test sensor that gradient noise does not degrade the measurements, but far enough apart that the stray fields of the test sensor do not significantly change the measurements of the witness sensors.

The materials used to make the magnetometer must be carefully selected to minimize heading error. One technical source of heading error is the field generated by ferromagnetic particles within the sensor. As the sensor's orientation is rotated, the permanent magnetic field of the particles also rotates, resulting in a variation of the total scalar field in the sensed volume. Manufacturers select nonmagnetic parts and then test the components for residual magnetism prior to construction. Another, generally smaller heading error arises from the diamagnetic materials and possibly also paramagnetic materials used to build the sensor and housing. These are polarized by the local magnetic field, and the induced field contributes to the field in the sensed volume. If these materials are unevenly distributed around the measurement cell, they will give rise to a net field which changes with heading, hence a heading error. Likewise these materials displace air, which includes paramagnetic oxygen. Displacing the oxygen changes the field in the sensed volume. Magnetic fields can also be generated by the sensor electronics. For example, a current loop of 10 mA with an area of 1 cm^2 generates a magnetic field of 7 pT at a distance of 30 cm. Electronic components may also be ferromagnetic. Careful construction of detection and amplification electronics is essential. Usually, the sensor electronics are separated from the atomic sensor itself, but on some measurement platforms it is impossible to separate the measurement from the electronics by more than 1 m.

Changes in the phase of the magnetometer's response result in heading errors when the magnetometer is operated in self-oscillating configuration. One source of heading error is the geometric-phase shift of the self-oscillating signal. Larmor precession is the result of the torque on the magnetic moment associated with the atomic spins, $\boldsymbol{\tau} = \boldsymbol{\mu} \times \mathbf{B}$ (Chapter 1). From the magnetometer's point of view, a 180° rotation is equivalent to a reversal of $\mathbf{B}$, hence a reversal of the precession. Such a phase reversal would change positive feedback needed to sustain self-oscillation into negative feedback. Commercial magnetometers automatically sense and correct electronically for the phase reversal to achieve continuous self-oscillation. However, at angles between 0° and 180°, the system can exhibit a smaller phase shift. This phase shift becomes a heading error as the feedback network dynamically changes

the self-oscillation frequency to maintain a zero net phase change around the feedback loop.

The nonlinear Zeeman (NLZ) effect can be a source of heading error (see Chapter 1, Section 1.1.2). The linear Zeeman effect provides a good approximation at Earth's field (about 3.5 Hz/nT for Cs, or 175 kHz at 50 μT), so that a single Larmor precession frequency is a useful concept. The NLZ effect causes the precession frequency to depend slightly (~7 Hz for Cs at 50 μT) on the direction of the atom's spin relative to the magnetic field; the NLZ effect becomes more pronounced at higher fields. The amplitudes for pumping and probing the atoms also depend on the direction of the atom's spin as well as the angles between the optical field and the magnetic field, so that as the heading changes, the relative strengths of the different components making up the signal change, thereby shifting the frequency at which the system self-oscillates. The net result is a heading error.

Another source of heading error is the inherent asymmetry of the signal when it is a composite of several hyperfine transitions (see also Chapter 4), for instance when atoms are probed with atomic emission lamps that contain a mix of optical wavelengths. The relative intensities of the unresolved hyperfine peaks depend on the heading angle. The result is that the self-oscillation frequency changes by ~10 nT. Balancing two beams with opposite circular polarization suppresses this heading error due to the virtual light shift to a fraction of a nT. Helium and potassium magnetometers operate on a single spectral line; hence they do not suffer from hyperfine-structure heading error. The heading error of commercial potassium magnetometers is typically 50 pT. Commercial He magnetometers have an intrinsic heading error of 600 pT, which is compensated to 80 pT.

20.2.10 Range of measurement

Commercial magnetometers are designed to measure the Earth's field over the entire surface of the Earth. The Earth's field varies from approximately 67 μT in Antarctica to as little as 22 μT in Brazil. The magnetometer must measure the total field value over this entire range (plus anomalies, e.g., 20 to 80 μT) with no increased drift or heading errors due to changes in the absolute field values. Some naturally occurring anomalies can exceed this range. For instance, the field in some parts of Brazil approaches zero, while ferrous outcroppings can result in surface fields of 500 μT.

Factors that affect the operation over this range of fields include changes in the spectroscopy of the atoms and performance issues related to the electronics. For the electronics, the main issue is balancing the wide bandwidth needed to handle a wide range of oscillation frequencies against the need to reduce noise by limiting the bandwidth. The primary physics issue is the NLZ splitting. If NLZ splitting is less than the linewidth of the magnetic resonance, then the NLZ effect will broaden the line. The broadening can lead to reduced signal-to-noise and possibly to heading errors as discussed above. For instance, when operating potassium magnetometers at fields as low as 20 μT, operation on one line is only possible by reducing the bandwidth of the measurement to ~85 Hz, as a result of the

decrease in the spread of the spectral lines. If the NLZ splitting is greater than the linewidth, then separate resonances can be observed, and it would be possible for the magnetometer to operate on any one of them. The range of Earth's field is sufficiently broad that some atomic systems can change from NLZ-unresolved to NLZ-resolved. Potassium and helium-4 magnetometers always operate with resolved NLZ (see Chapters 4 and 10, respectively). The magnetometer must operate properly over the full Earth-field range.

20.3 History of commercial magnetometry

20.3.1 Fluxgate magnetometers

Although neither a quantum nor an optical magnetometer, the fluxgate magnetometer merits discussion in this chapter because it has historically been used for similar applications as optical magnetometers. The fluxgate magnetometer was originally developed in the 1940s for use in anti-submarine warfare and after World War II was adopted for airborne geophysical surveys for natural-resource exploration.

A fluxgate magnetometer usually consists of a series of windings around a ferromagnetic core in which the permeability is a function of field strength. The windings are used to impress both an AC and a DC field on the core, in addition to the ambient field. The AC driving signal is used to drive the core through saturation around its hysteresis loop. The ambient field adds to the AC field in one half-cycle and subtracts in the other, creating a difference in the interval of saturation, detectable at twice the driving frequency using lock-in detection techniques for added sensitivity. This rectified asymmetry signal is proportional to the vector component of the ambient field along the AC field, although the constant of proportionality depends on the details of the nonlinear response of the core. The applied DC field is adjusted to null the ambient field. The current used to produce the DC field measures the ambient DC field and is independent of the core nonlinearity.

A number of fluxgate instruments have been developed. In its various configurations, the instrument is known as a second-harmonic, ring core, thin film, or oriented fluxgate magnetometer. The DC current used to null the ambient field is a source of some instability at long periods but careful design allows sensitivity of perhaps 0.05 nT in recently developed instruments, 0.1 nT in some of the airborne and monitoring versions, and 0.5 nT for hand-held portable instruments.

All fluxgate magnetometers measure a relative rather than absolute value of the magnetic field and as such must be calibrated in some way. A reference atomic magnetometer is commonly used to calibrate the fluxgate in airborne, satellite, and some ground survey applications. Since the fluxgate measures a vector component of the field, survey applications require that the instrument be referenced to some spatial coordinate system such as vertical, as in the case of ground portable surveys, or electromechanically oriented along the Earth field for airborne surveys. Archaeological survey in many parts of the world employ high-performance, low-drift multiple vertical fluxgate gradiometer arrays, providing excellent near-surface (short-range) anomaly detection.

Oriented fluxgate systems utilize three mutually orthogonal fluxgate sensors that are continuously oriented by a remote motor so that two of the sensors measure zero field. The third or primary sensor thus measures the maximum vector, otherwise referred to as total magnetic intensity. The precision of the sensors and the electromechanical orientation system are some of the principal limitations on sensitivity or resolution, particularly on a rapidly moving platform. Most satellites, a few airborne research survey aircraft, and some borehole probes utilize three mutually orthogonal fluxgate sensors referenced to an inertial or other spatial coordinate system in order to obtain vector information of the field. The periodic rotation of a satellite can be used to process fluxgate readings to reduce the effect of errors from drifting calibrations in the x, y, and z axes.

20.3.2 SQUID magnetometers

The superconducting quantum interference device (SQUID) magnetometer has the highest sensitivity of any commercial magnetometer. The SQUID magnetometer is based on Josephson's discovery in the early 1960s that small gaps in a circulating superconducting current loop were sensitive to magnetic flux perpendicular to the loop causing changes in the current flow. A resonant circuit is used to monitor the current changes and obtain vector-field information. SQUIDs are very sensitive ($\sim 3 \times 10^{-14}$ T), high-bandwidth (up to 50 kHz) devices [6]. The advent of high-temperature superconductors increased the usefulness of SQUIDs for geophysical surveys, although these devices have higher noise than low-temperature SQUID magnetometers. SQUID sensors have commercial applications in biomagnetics (heart and brain monitoring), magnetotellurics (measuring electrical currents flowing in the earth), and in paleomagnetics (where rock samples are measured for remanent field direction and density, demagnetized, then re-measured to determine the sample's chronological magnetic history). Recently SQUID sensors have also been used for stationary electromagnetic surveys as magnetic current sensors. However, SQUIDs are rarely used with mobile platforms due to a variety of practical limitations. The need for cryogenic cooling creates logistic difficulties for deploying SQUID sensors, because cryogenic fluids such as liquid nitrogen or liquid helium are not widely available. Motion of the sensor platform reduces the usefulness of vector sensors. Using three orthogonal SQUID sensors could in principle provide the total scalar field but, in practice, maintaining the relative orientation of the three sensors to the accuracy required to match the extraordinary sensitivity of the SQUID is a formidable challenge. Finally, SQUID sensors are several times more expensive than proton or alkali-vapor magnetometers. Thus, SQUID sensors tend to dominate only in markets where the highest sensitivity is critical for successful measurements.

20.3.3 Proton-precession and Overhauser magnetometers

The proton magnetometer was developed by Varian and Packard in 1954 as an outgrowth of research involving nuclear magnetic resonance [7]. The proton magnetometer, also called nuclear-precession, proton-precession, or proton free-precession magnetometer, consists of

a coil of wire surrounding a fluid containing hydrogen atoms such as water, kerosene, etc. The proton is itself a magnetic dipole that can be polarized by applying a magnetic field at right angles to the field to be measured, which is produced by a DC current in the coil surrounding the sample. After the current in the coil is abruptly terminated, these spinning protons precess about the direction of the ambient magnetic field, at a frequency that is proportional to the field intensity. The precessing protons induce a signal, typically, 2 kHz, in the polarizing coil. The polarization usually decays in a matter of a few seconds, requiring a repolarization between measurements, and the measurements are thus discontinuous. Commercial magnetometers are operated at a rate of up to several readings per second.

Proton magnetometers, in common with atomic magnetometers, measure spin precession to determine the total scalar magnetic field. This characteristic facilitates magnetic survey applications on a moving platform because the sensor measures magnetic field independently of its orientation. As a result, precession-based magnetometers are widely used for ground, marine, and airborne surveys.

A variation of the proton magnetometer, the Overhauser or Abragam magnetometer, uses an organic hydrocarbon fluid containing free radicals that can be polarized by a (linearly polarized) radiofrequency exciting field whose frequency is appropriately adjusted. The free radical transfers its polarization to the proton sample. The Overhauser-effect magnetometer provides a continuous measurement. Because Overhauser magnetometers do not require a DC polarizing field, the exciting field (about 60 MHz) does not degrade the absolute accuracy of Overhauser magnetometers.

Commercial proton-precession magnetometers appeared in the early 1960s. Breakthroughs led to sensitivities of single-digit nT and then fractions of a nT; the improvements were immediately applied in mineral exploration. Geometrics [8] optimized the technology and used it in airborne surveys. A team in Grenoble, France, developed a continuous proton oscillator based on the Overhauser effect for military magnetic-anomaly detection [9]. Canadian development followed with similar continuous-precession magnetometers by Scintrex in 1970 [10]. GEM Systems [11] developed continuous and pulsed versions in the early 1980s. Sensors from these manufacturers achieved up to 5 readings/s and about 0.02 nT sensitivity.

The maximum sensitivity of commercial magnetometers based on proton precession of either type is generally 0.01 nT. The absolute accuracy of the free-precession magnetometer, however, is approximately 0.1 nT. This represents an absolute error of about 2 ppm in a field of 50 μT. The accuracy is limited primarily by the magnetic properties of the sensor, accuracy of the frequency-counting circuits, and known precision of an atomic constant. At present the proton-precession magnetometer provides the most accurate measurement of the absolute value of the Earth's magnetic field of any commercial magnetometers. The standard for magnetic observatories for scalar total-field measurement is an Overhauser proton-precession magnetometer with sensitivity of about 10–20 pT, absolute accuracies of $\pm$0.1 nT, and a 1 Hz measurement rate. The frequency response of commercial proton magnetometers is limited by the highest cycle rate to a few Hz for free-precession or

Overhauser instruments. Proton magnetometers will not operate in high gradients, which limit their use in some ground surveys, such as over iron formations.

20.3.4 Alkali metal magnetometers: rubidium, cesium, and potassium

The optically pumped rubidium magnetometer was first used for geophysical measurements in 1957 [12]. Manufacturers included Varian, which later sold its magnetometer product line to CAE for military use and to Scintrex for commercial use. Early optically pumped magnetometers utilized a lamp containing the alkali metal. Light from the lamp passed through a glass cell containing the vapor of the same element and was focused on a photodetector on the other side of the vapor cell. In recent decades, diode lasers of the proper frequency have been developed to excite the atoms in the vapor cell, but many commercial instruments still use a lamp as the light source. The output of the photodetector is connected through an amplifier to a coil surrounding the vapor cell. This electro-optic system, through resonant absorption and re-radiation of energy, constitutes an oscillator whose frequency is directly proportional to the scalar magnetic field intensity in much the same way as for the proton-precession magnetometer. But where the proton-precession magnetometer operates in pulsed mode, optically pumped magnetometers typically operate with a continuous signal. The signal frequency is higher, roughly as the ratio of the electron mass to the proton mass: several hundred kHz for the alkali metals and 2 MHz for helium. The time response of the magnetometer is governed by the time interval over which the oscillation frequency is counted; practical devices can have kHz update rates.

The sensitivity of a cesium magnetometer has been shown to be 0.5 pT in a bandwidth of approximately 0.1 Hz through 10 Hz and possibly 1 pT between 10^{-3} Hz and 100 Hz. The absolute accuracy of a conventional optically pumped magnetometer, however, is generally 1 nT to several nT due to the complexity of various resonant lines on which it operates that in turn are a function of orientation in the Earth's magnetic field and several operating characteristics of the exciting lamp and amplifier.

Potassium narrow-spectral-line magnetometers appeared as a result of cooperation between the St. Petersburg research group led by Dr. E. B. Alexandrov and the Canadian manufacturer GEM Systems. The hyperfine structure of potassium (K) reduces certain heading-error effects and results in better absolute accuracy. The vapor pressure of potassium is lower than that of cesium at a given temperature, so typically potassium-based sensors must be heated, resulting in somewhat higher power consumption. Development has now resulted in a single-spectral-line operation and a sensitivity of some 30 fT once per second in stationary installations and about 0.1 pT in mobile applications. High absolute accuracy is obtained, similar to proton/Overhauser magnetometers.

The smaller intrinsic heading error of K means split-beam operation is not necessary to cancel it. This results in somewhat simpler electronics. The high sensitivity and small heading error make the K magnetometer a good fit for multiple-sensor applications. Potassium is now used in helicopter-borne and fixed-wing-craft-borne gradiometers and in ground surveys requiring superior sensitivity and gradient tolerance.

20.3.5 Helium-3 and helium-4 magnetometers

The innovation leading to helium magnetometers began with the first optical pumping of the metastable level of helium by Colegrove and Franken at the University of Michigan in 1958 [13]. The Franken patent [14] was purchased by Texas Instruments in 1959 leading to the first optically pumped scalar helium magnetometer at Texas Instruments (TI) in 1960 [15]. The TI team produced more than 1500 scalar He-4 magnetometers based on this technology for use by the US Navy for airborne magnetic-anomaly detection (MAD) of submarines. Lamp-pumped He-4 magnetometers were independently developed and manufactured beginning in the 1960s by Sinclair Research (later a part of ARCO) [16] and in the 1990s by China's Aero Geophysical Survey & Remote Sensing Center for Land and Resources (AGRS) [17].

Colegrove, Walters, and Schearer demonstrated a method for spin-exchange optical pumping of metastable helium atoms to create spin-polarized He-3 nuclei [18, 19], which led to the development of the He-3 nuclear free-precession magnetometer by Slocum and Marton in 1974 [20]. The first space vector-helium magnetometer was developed at TI in 1961 and is described in Chapter 10 [21]; a series of seven space magnetometers for Earth, planetary, and solar missions, built at the NASA Jet Propulsion Laboratory (JPL), followed. The ARCO–Sinclair magnetometer was not marketed but was used for in-house aeromagnetic surveys for oil and mineral exploration. AGRS also used helium magnetometers for aerial magnetic surveys.

All He-4 magnetometers manufactured in the twentieth century were lamp-pumped instruments from TI, JPL, and two geophysical-exploration organizations. The switch to laser pumping resulted in a significant advance in sensitivity of He magnetometers. In the USA, Polatomic [22] was founded by R. E. Slocum in 1982 and pursued practical application of 1083 nm semiconductor DBR laser pump sources for high-performance He-4 and He-3 magnetometers. One important application was the development of the next-generation laser-pumped AN/ASQ-233 He-4 system for US Navy anti-submarine aircraft, with research and development funding provided through the Small Business Innovation Research (SBIR) Program. The development of laser-pumped helium magnetometers over the last two decades resulted from a collaboration of four institutions: Polatomic, Inc., L. D. Schearer of the University of Missouri-Rolla in the USA, M. Leduc and F. Laloe of the Ecole Normale Superieure, Paris, and J. M. Hamel of the ISMRA at Caen, France. This effort included development of laser pump sources for He isotopes [23], applications of laser-pumped helium isotopes, and magnetometers using He-3 and He-4. In 1996, LETI-CEA Advanced Technologies, Grenoble, France, was selected to design and build a laser-pumped He-4 magnetometer for the SWARM satellites. At the time of writing this was scheduled for launch no earlier than November 2012. The SWARM instrument is discussed in detail in Chapter 15.

Helium-magnetometer technology has tended to emerge from government and corporate-sponsored R&D activities without a commercial outlet in North America and Europe. Alkali-vapor magnetometers have seen multiple commercial outlets as well as government-sponsored development. There has been surprisingly little interaction between

the two groups over the past 50 years, with an intangible "repulsion factor" that seems to be based on research culture as much as technology. Following the invention of optical pumping of He-4 by Colegrove and Franken, the helium optical pumping patent was offered to Varian by Peter Franken. He reported that his friends at Varian would be happy to buy it but that they would only put it "on the shelf," because they were pleased with and committed to Rb and other alkali-vapor instruments. Franken immediately sold the patent in 1959 to Texas Instruments, who ten years later won the competition with Varian for the next-generation US Navy airborne AN/ASQ-81 MAD system, a contract which totaled approximately $1 billion in sales in today's dollars. In 1981 Varian made an offer to sell its alkali-vapor magnetometer business to TI, which would bring the manufacture of alkali and helium magnetometers under one roof, but the offer was declined. Meanwhile in the 1980s, EG&G owned Geometrics and considered purchasing a startup laser-helium-magnetometer company, Polatomic, but instead made an offer to sell Geometrics' alkali-vapor-magnetometer business to Polatomic, an offer that also was declined. Following a merger of its business unit with Raytheon in 1997, the Texas Instruments Defense Group exited the magnetometer-manufacturing business, whereupon a large part of the helium magnetometer technical team migrated from TI to Polatomic. Because the technology for making helium and alkali-vapor magnetometers has remained in separate companies, there is no optical magnetometer "superpower." A healthy magnetometer competition continues today.

20.4 Military applications

Important military applications that use atomic magnetometers include magnetic-anomaly detection (MAD) for both anti-submarine warfare (ASW) and for locating mines and unexploded ordnance (UXO). Other applications where atomic magnetometers might be useful include perimeter monitoring and detection of improvised explosive devices (IEDs).

The US Navy flies magnetic-anomaly-detection systems in the tail stinger of a P-3 Orion aircraft based on the AN/ASQ-81 and AN/ASQ-208 magnetometers. Combined sales amounted to about 1500 units at a unit cost of $350 000 (1991 dollars) [24]. Typically the MAD system will include one or more atomic magnetometers, a less-accurate vector magnetometer for correcting heading errors that arise in the atomic magnetometer and from the magnetic field of the aircraft, and motion sensors that can be used to compensate for the apparent signal due to spatial variations in Earth's field. The P-3 flies localization patterns at about a hundred meters above sea level. The Navy prefers scalar magnetometers for airborne magnetic-anomaly detection because the scalar measurement is less susceptible to orientation errors arising from the motion of the aircraft.

The P-3 platform was introduced in the late 1950s. The US Navy is presently investigating other options for airborne magnetometry, such as unmanned aerial vehicles (UAVs). Unmanned platforms can stay on patrol for longer periods of time and relieve flight crews of the drudgery of flying search patterns. Typically the craft are much smaller than the P-3, so instruments must be lighter and consume less electrical power. The smaller physical separation of the sensor from the body of the UAV may require improvements in algorithms for compensating for platform noise.

Underwater surveys of the seafloor are important in military and commercial applications. Although an unmanned underwater vehicle (UUV) requires an up-front capital cost, it provides significant savings in operating cost for near-seafloor surveys, especially in deep water. Taking into account the time it takes to turn around a deep-tow marine magnetometer system, a UUV can complete a deep-water survey in one quarter of the time it takes a surface ship towing an array to cover the same area. The UUV also can operate at greater depth, closer to targets buried on the seafloor [25].

20.5 Anticipated improvements

The future market for quantum magnetometers will be shaped by several forces. First, users will increasingly migrate to small, automated platforms such as UAVs for airborne sensing and UUVs for underwater exploration. These platforms in turn require smaller, lower-power sensors and improved rejection of platform noise. Second, new technologies may allow significant improvement in sensitivity or other performance parameters [26]. A new company, Twinleaf [27], was formed to commercialize some of these improvements. Another company, Southwest Sciences [28], has developed fiberized magnetometers for characterizing magnetic fields inside magnetic shields. Existing companies continue to upgrade their products by introducing promising new technologies.

New applications will demand improved performance. High-performance potassium gradiometers have recently been installed in Mexico, in Israel, and at a fixed magnetic observatory in Austria. Other high-sensitivity gradiometers are used for earthquake studies, magnetotellurics, and ionospheric measurements. In addition to high sensitivity, magnetometers for such gradiometers require high immunity from heading error, so that lower-order fields do not contaminate the measurement of gradients. Another new application uses an array of sensors to produce magnetic maps much more quickly. Commercial success hinges on reducing the cost of the sensor array significantly below the cost of a similar number of stand-alone instruments.

Surveys for unexploded ordnance (UXO) or improvised explosive devices (IEDs) are clear examples of dangerous endeavors. Robots carrying high-sensitivity magnetometers, perhaps configured in multiple-sensor arrays, can conduct these type of surveys efficiently with no danger to human life. As with all robotic magnetometer installations, careful and innovative compensation techniques will be required to minimize not only the induced, remanent, and eddy-current sources of noise but also noise generated by the control electronics, other sensors, or motive power and propulsion-system components. Currently work is underway to automate compensation for all these noise sources.

References

[1] J. M. Higbie, E. Corsini, and D. Budker, Rev. Sci. Instrum. **77**, 113106 (2006).
[2] I. Hrvoic, in *Proceedings of the VIth workshop on geomagnetic observatory instruments, data acquisition and processing*, edited by J. L. Rasson (Institut Meteorologique du Belgique, Brussels, 1994), pp. 70–72; available at gemsys.ca.

[3] P. J. Mohr, B. N. Taylor, and D. B. Newell, Rev. Mod. Phys. **80**, 633 (2008); values are tabulated in NIST Reference on Constants, Units and Uncertainty, http://physics.nist.gov/cgi-bin/cuu/Value?gammap.
[4] D. A. Steck, *Cesium D Line Data*, published online at http://steck.us/alkalidata/cesium-numbers.pdf.
[5] S. Pustelny, D. F. Jackson Kimball, S. M. Rochester, V. V. Yashchuk, and D. Budker, Phys. Rev. A **74**, 063406 (2006).
[6] M. N. Nabighian, V. J. S. Grauch, R. O. Hansen, T. R. LaFehr, Y. Li, J. W. Peirce, J. D. Phillips, and M. E. Ruder, Geophysics **70**, 33ND (2005).
[7] M. Packard and R. Varian, Phys. Rev. **93**, 941 (1954).
[8] Geometrics, San Jose, CA, USA; www.geometrics.com.
[9] G. Bonnet, J. L. Laffon, and P. Servez-Gavin, United States Patent 3,133,243 (May 12, 1964).
[10] Scintrex Limited, Concord, ON, Canada, www.scintrexltd.com.
[11] GEM Systems, Markham, ON, Canada, www.gemsys.ca.
[12] T. L. Skillman and P. L. Bender, J. Geophys. Res. **63**, 513 (1958).
[13] F. D. Colegrove and P. A. Franken, Phys. Rev. **119**, 680 (1960).
[14] P. A. Franken, United States Patent 3,122,702 (February 25, 1964).
[15] A. R. Keyser, J. A. Rice and L. D. Schearer, J. Geophys. Res. **66**, 4163 (1961).
[16] R. E. Hartline and F. H. Meister, US Patent 3,513,383 (May 19, 1970).
[17] Aero Geophysical Survey and Remote Sensing Center, China (AGRS), http://www.agrs.cn/cms/website/english/.
[18] G. K. Walters, F. D. Colegrove, and L. D. Schearer, Phys. Rev. Lett. **8**, 439 (1962).
[19] F. D. Colegrove, L. D. Schearer, and G. K. Walters, Phys. Rev. **132**, 2561 (1963).
[20] R. Slocum and B. Marton, IEEE Trans. Magn. **10**, 528 (1974).
[21] R. E. Slocum and F. N. Reilly, IEEE Trans. Nucl. Sci. **NS-10**, 165 (1963).
[22] Polatomic, Inc., Richardson, TX, USA, www.polatomic.com.
[23] L. Schearer, M. Leduc, F. Laloe, and J. M. Hamel, United States Patent 4,806,864 (February 21, 1989).
[24] Forecast International, *ASQ-81(V)/ASQ-208(V) ASW forecast* (February 2003).
[25] G. I. Allen, G. Sulzberger, J. T. Bono, J. S. Pray, and T. R. Clem, Proc. MTS/IEEE **3**, 1956 (2005).
[26] D. Budker and M. Romalis, Nature Physics **3**, 227 (2007).
[27] Twinleaf, Princeton, NJ, USA, www.twinleaf.com.
[28] Southwest Sciences, Inc., Santa Fe, NM, USA, www.swsciences.com.